ngVLA Memo #21

ngVLA Sensitivity

Bryan Butler, Wes Grammer, Rob Selina, Eric Murphy, Chris Carilli

National Radio Astronomy Observatory

June 27, 2019

1 Introduction

The design for the next generation Very Large Array (ngVLA) is now mature enough to make a much more detailed calculation of sensitivity than has been possible before. Previous estimates (e.g., Carilli et al. 2015; Selina & Murphy 2017) have suffered from uncertainties in design specifics, some of which have been reduced through further development. Furthermore, it is of interest to compare these sensitivity numbers directly with existing and near-future instruments in the frequency range of ngVLA (1.2 to 116 GHz), namely the current Karl G. Jansky Very Large Array (VLA), the Atacama Large Millimeter/submillimeter Array (ALMA) and the Square Kilometer Array phase 1 (SKA1-mid). We base our sensitivity calculation on the one for ALMA presented in Butler & Wootten (1999), with modifications, along with current best estimates of receiver and antenna performance, combined with atmospheric models based on measured VLA site characteristics.

2 Point source sensitivity

For an unresolved source, the rms noise ΔS at frequency ν (and observed over the frequency range ν_1 to ν_2 with bandwidth $\Delta\nu = \nu_2 - \nu_1$) can be written:

$$\Delta S(\nu) = \frac{4\sqrt{2}k}{\pi D^2 \sqrt{n_p \left[N\left(N-1\right)/2\right] \Delta\nu \Delta t}} \frac{1}{\Delta\nu} \int_{\nu_1}^{\nu_2} \frac{T_{sys}\left(\nu\right)}{\eta_a\left(\nu\right)} d\nu \quad \left[\mathrm{W/m^2/Hz}\right] \qquad (1)$$

where k is Boltzmanns constant, T_{sys} is the system temperature, η_a is the antenna efficiency, D is the antenna diameter, n_p is the number of simultaneously sampled polarizations, N is the number of antennas in the array, and Δt is the integration time. Note that we have assumed that the "gridding parameter" and the correlator efficiency that are included in Butler & Wootten (1999) are both 1.0.

2.1 Parameters taken as fixed

We assume that the ngVLA is comprised of 214 18-m diameter antennas, so $D = 18$; $N = 214$. Note that we are not considering the addition of the Long Baseline Array antennas (30 18-m antennas) or the smaller Short Baseline antennas (19 6-m antennas) in this treatment. We assume dual-linear polarization so $n_p = 2$. Given these assumptions, equation 1 above reduces to:

$$\Delta S(\nu) = \frac{35.9}{\sqrt{\Delta\nu \Delta t}} \frac{1}{\Delta\nu} \int_{\nu_1}^{\nu_2} \frac{T_{sys}\,(\nu)}{\eta_a\,(\nu)} d\nu \qquad \text{[mJy]} \tag{2}$$

We assume 6 receiver bands covering the range from 1.2 to 116 GHz, with frequency ranges of: 1.2-3.5 GHz; 3.5-12.3 GHz; 12.3-20.5 GHz; 20.5-34 GHz; 30.5-50.5 GHz; and 70-116 GHz; denoted as bands 1 through 6. For continuum sensitivity calculations we assume bandwidths that are either the entire band, or 20 GHz for band 6.

2.2 Antenna efficiency

Antenna efficiency is a combination of several terms, including feed illumination efficiency, surface efficiency (Ruze losses), and potentially other terms (for instance, for a symmetric Cassegrain telescope there will be a subreflector blockage term) (Napier 1998). We include here only feed illumination efficiency and surface efficiency (the current antenna design has an unblocked aperture). The surface efficiency is calculated via (Ruze 1952):

$$\eta_{surf} = e^{-\left(\frac{4\pi\sigma}{\lambda}\right)^2} \tag{3}$$

for surface error σ and wavelength λ. The current design specification for the ngVLA antenna surface is $\sigma = 160$ μm (under precision operating conditions), and we use that value, but

we also include a calculation below where we use the value for non-precision conditions (σ = 300 μm) for bands 1-5. For bands 1 and 2 we take the feed illumination efficiency from Weinreb & Mani (2017). For bands 3 through 6 we take this efficiency from Baker (2018), scaled to the appropriate frequencies (see also Baker & Veidt 2014). The values are tabulated in detail in Table 2 of Grammer & Durand (2019).

Figure 1 shows the antenna efficiency over the entire frequency range of interest, along with fits used in evaluating the integral in equation 1, for both precision and non-precision conditions.

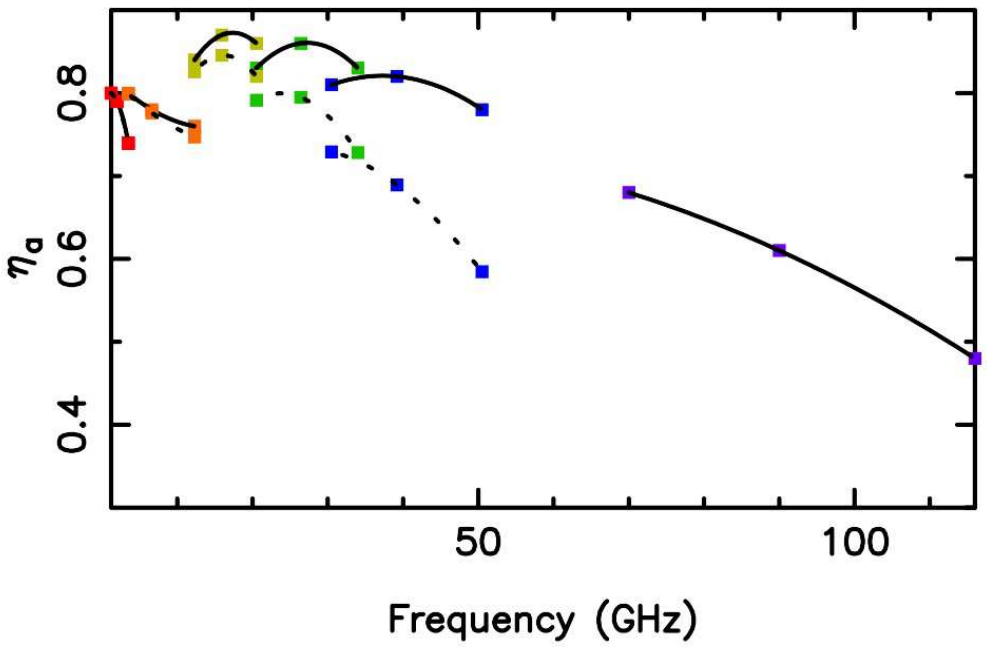

Figure 1: Estimated antenna efficiency for ngVLA antennas and feeds for band 1 (red), band 2 (orange), band 3 (yellow), band 4 (green), band 5 (blue), and band 6 (purple). Fits to be used in the evaluation of equation 1 are also shown. The solid lines show the values and fits under precision conditions; the dashed lines for non-precision (we assume band 6 will not be observed under non-precision conditions).

2.3 System temperature

Refer T_{sys} to a point outside the atmosphere and compute it as:

$$T_{sys}(\nu) = \alpha T'_{rx} + \alpha \eta_l T'_{atm} + \alpha T'_{spill} + T'_{bg} \qquad \text{[K]} \tag{4}$$

where $\alpha = e^{\tau}$ is an atmospheric absorption correction for opacity τ, T'_{rx} is the receiver temperature, η_l is the fraction of the antenna power that is received in the forward direction (i.e., the fraction that is on the sky in the main lobe and all the forward sidelobes; we assume $\eta_l = 0.97$), T'_{atm} is the effective atmospheric temperature, T'_{spill} is the spillover temperature and T'_{bg} is the background temperature. The terms of Tsys in equation (3) represent contributions from the receiver, the atmosphere, the "antenna," and the background. The primes on the temperatures indicate that they are effective radiation temperatures, and should be calculated with a Planck correction (Ulich & Haas 1976):

$$T'_x = \frac{h\nu/k}{e^{h\nu/kT_x} - 1} \tag{5}$$

where ν is the frequency, and T_x is the physical temperature. This can make a sizable difference in band 6 for low temperatures.

2.4 T_{rx}

We calculate T_{rx} by taking contributions from the LNA, receiver, cal coupler, feed, window, IR filter, post-amplifier, and coaxial losses, given our current baseline design for the receiver package. The values are tabulated in detail in Table 2 of Grammer & Durand (2019). Figure 2 shows a plot of the values of T_{rx} as a function of frequency, along with fits which can be used in evaluating the integral in equation 1.

2.5 T_{atm} and τ

We calculate T_{atm} and τ by creating model atmospheres (pressure, temperature, and water vapor content as a function of altitude above ground) and integrating to find the quantities. We use the atmospheric model of Liebe (1989) for this. The whole process is described in great detail in Butler (1999). To create the model atmosphere, the surface pressure, temperature, and total precipitable water vapor (PWV) must be known. Given the large area covered by ngVLA (at least 500 km in extent), these quantities will vary at any given time across the array, but we assume that the VLA site is a decent proxy site. The temperature

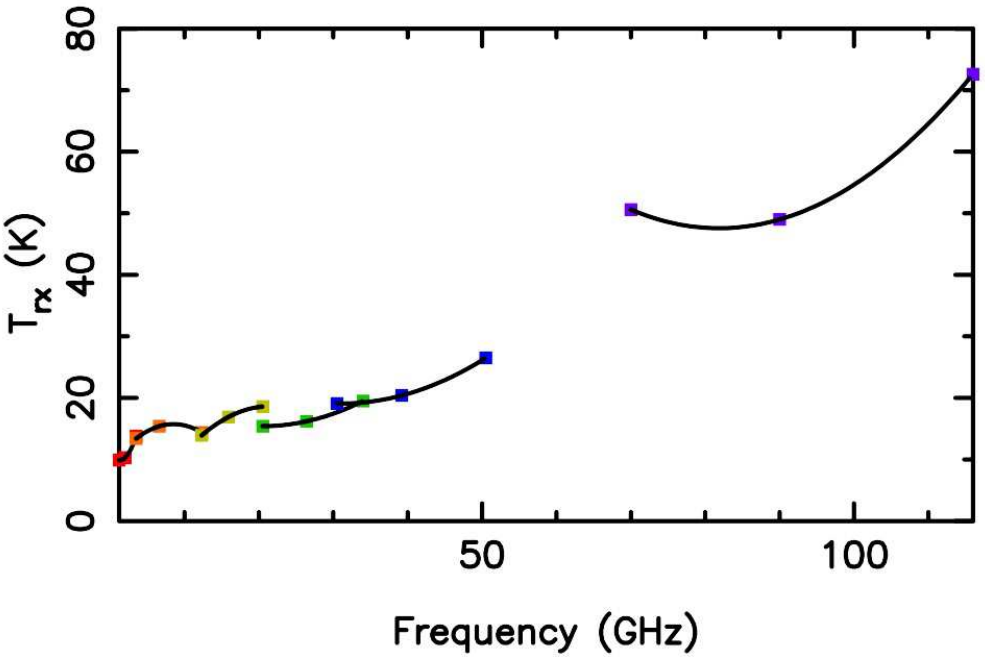

Figure 2: Estimated receiver temperature for ngVLA receivers for band 1 (red), band 2 (orange), band 3 (yellow), band 4 (green), band 5 (blue), and band 6 (purple). Fits to be used in the evaluation of equation 4 are also shown.

and PWV are not only areally variable, but are also strongly variable as a function of season and time of day. By contrast, the surface pressure has only little variation - of order 1%, over time, which we ignore. We have measurements of surface temperature (T_{surf}) at the VLA site going back 40 years, but we will use only measurements in the past 7 years. Figure 3 shows a plot of T_{surf} over this period. In order to reduce parameter space, we take two representative periods, winter and summer, considered to cover the periods from December 1 to February 28 (or 29) and June 1 to August 31 for each year. We refer to these periods and their associated values as "dry" and "wet" subsequently. We take the medians of all values shown in Figure 3 for those periods, 274 K for dry and 293 K for wet, and perform our calculations using model atmospheres with those values of T_{surf}.

Given surface meteorological measurements, the precipitable water vapor (PWV) can be calculated (Butler 1998a, 1998b). Figure 4 shows a plot of derived PWV over the 2010-2017 time period. We use the medians of these values over the periods noted above, 4 mm and 18 mm for dry and wet conditions, respectively, for our model atmospheres (note that these

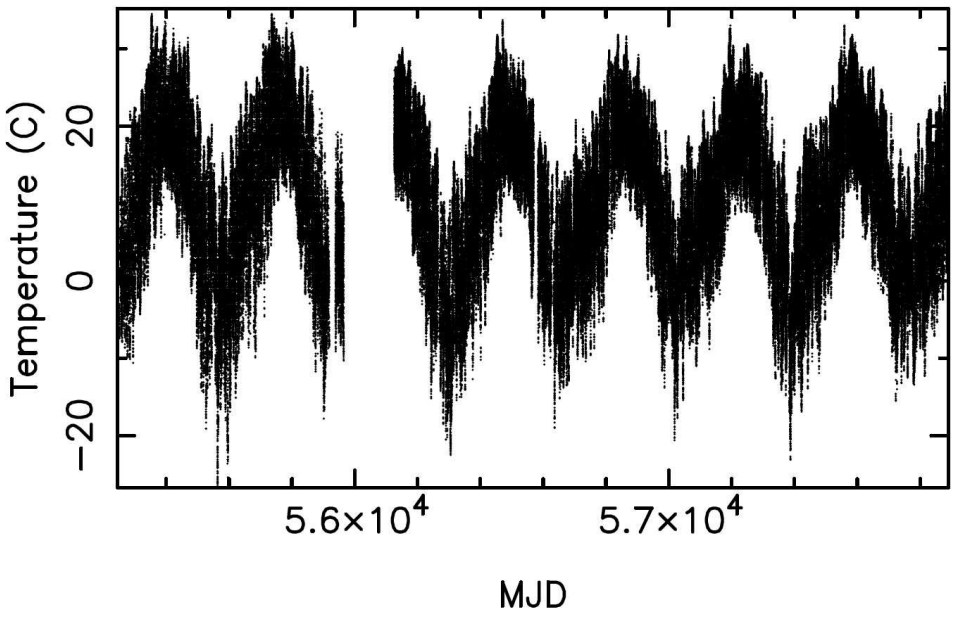

Figure 3: Surface temperature at the VLA site from 2010-2017.

are close to median values in Butler 1998b for the appropriate months; the difference can be ascribed to the fact that our weather instrumentation at the VLA has improved in accuracy since that old analysis was done).

With values of surface temperature and PWV, model atmospheres are created and values of T_{atm} and τ can be derived as a function of frequency. We calculate these values using a moderate elevation of 50 degrees. These are shown in Figure 5.

2.6 T_{spill}

Spillover includes the contribution to system temperature from directions outside the main beam of the antenna. It comes from a number of causes, including diffraction, multiple reflections, etc. Traditionally it has been considered to be that fraction of the radiation pattern that falls on the ground (instead of "cold sky"), but this is a simplistic way of considering it. We have modeled the spillover temperature based on simulations from Srikanth (personal communication), based on the current antenna optics and feed designs. The values are tabulated in detail in Table 2 of Grammer & Durand (2019). Figure 6 shows a plot of the values of T_{spill} as a function of frequency, along with fits which can be used in evaluating

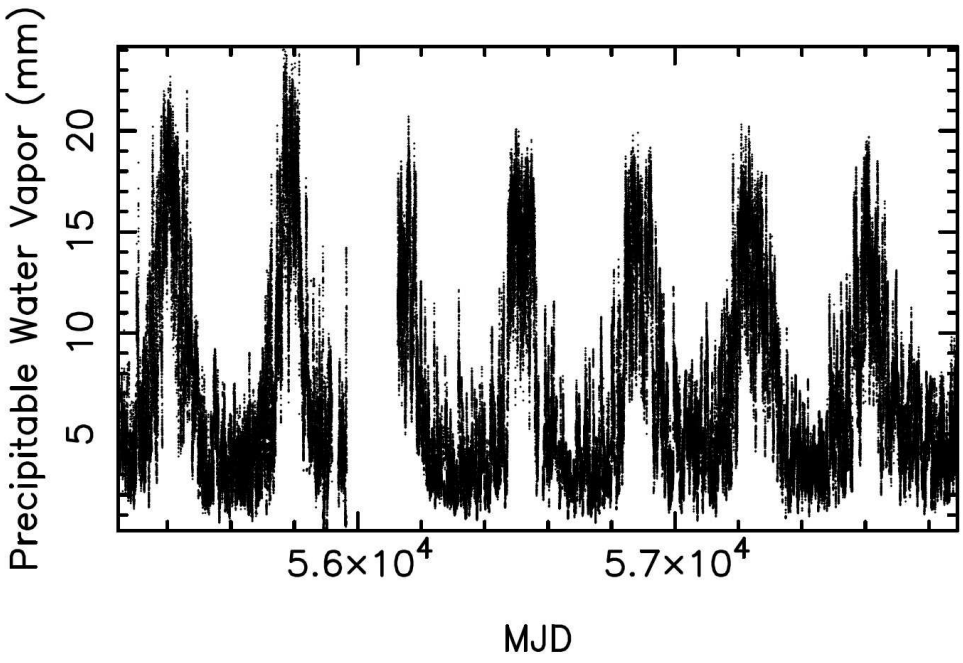

Figure 4: Precipitable Water Vapor (PWV) at the VLA site from 2010-2017.

the integral in equation 1.

2.7 T_{bg}

The background temperature comes from two sources: the cosmic microwave background, and galactic background. We use 2.725 K for the cosmic microwave background. For the galactic contribution, we use $T_{gal} = 25.2(0.408/\nu_{GHz})^{2.75}$ K for frequency ν_{GHz} in GHz, which is a rough average over the sky (away from the galactic plane). The galactic contribution is only significant at the lower end of band 1 (T_{gal} at 1.2 GHz 1.3 K).

3 Results

We calculate the continuum point source sensitivity given the above information over bands 1-5 over their entire extent, and two values for band 6 (70-90 GHz and 95-115 GHz). The integration time (t) is taken to be 1 hour. Results are shown in Table 1.

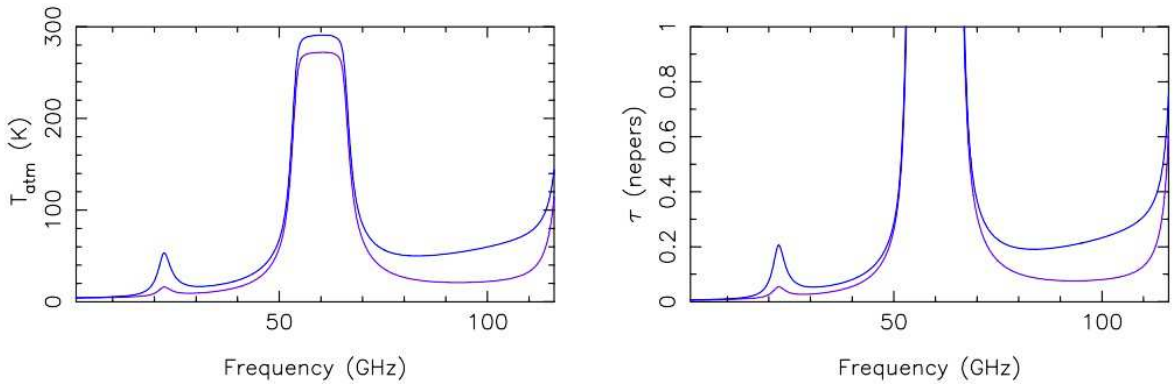

Figure 5: Atmospheric temperature (left) and opacity (right) at the VLA for wet (blue) and dry (purple) conditions.

Table 1: ngVLA continuum sensitivity in 1 hour.

band	frequency range (GHz)	precision dry sensitivity (μJy)	precision wet sensitivity (μJy)	non-precision dry sensitivity (μJy)	non-precision wet sensitivity (μJy)
1	1.2-3.5	0.438	0.438	0.438	0.438
2	3.5-12.3	0.239	0.242	0.240	0.244
3	12.3-20.5	0.232	0.272	0.240	0.282
4	20.5-34.0	0.215	0.328	0.234	0.356
5	30.5-50.5	0.288	0.340	0.356	0.419
6	70.0-90.0	0.637	0.884	–	–
6	95.0-115.0	0.871	1.432	–	–

3.1 Frequency response (spectral line)

To examine the details of the sensitivity as a function of frequency, we can form a monochromatic sensitivity quantity:

$$\Delta S'(\nu) = \frac{N\pi D^2 \eta_a(\nu)}{4T_{sys}(\nu)} \qquad [\mathrm{m}^2/\mathrm{K}] \tag{6}$$

This is an appropriate quantity for examining the spectral line sensitivity as a function of frequency. Figure 7 plots this quantity for the ngVLA.

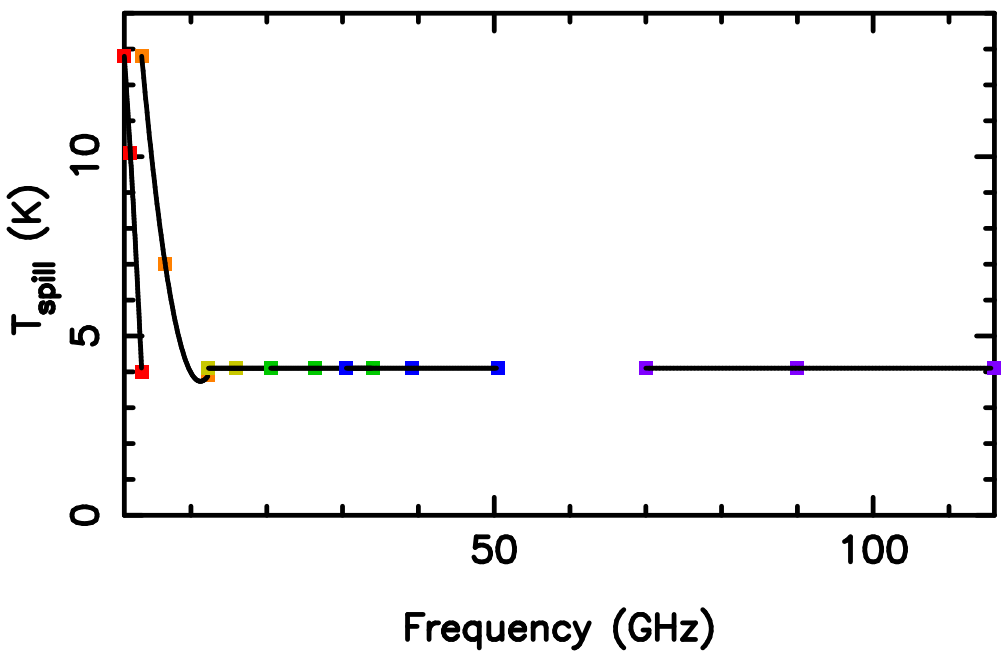

Figure 6: Estimated spillover temperature for ngVLA receivers for band 1 (red), band 2 (orange), band 3 (yellow), band 4 (green), band 5 (blue), and band 6 (purple). Fits to be used in the evaluation of equation 4 are also shown.

3.1.1 Comparison to other facilities

Using equation 6 we can perform a similar calculation for current VLA, current ALMA and planned SKA1-mid for frequencies that overlap with those of ngVLA (bands L- through Q- for VLA; band 3 for ALMA; bands 2-5+ of SKA1-mid).

VLA

For the VLA, we use measured values of the SEFD at zenith to calculate $\Delta S'$, but add a correction factor to account for observing at 50 degrees elevation, and for atmospheric absorption. In principle this correction factor is a strong function of band, specific frequency, and atmospheric conditions, but we use a constant factor of 1.25 for simplicity. This is too large at low frequencies and too small at high frequencies, but is sufficient for this analysis. We use the values of SEFD which are incorporated into the VLA Exposure Calculator Tool, which have been measured on the actual array.

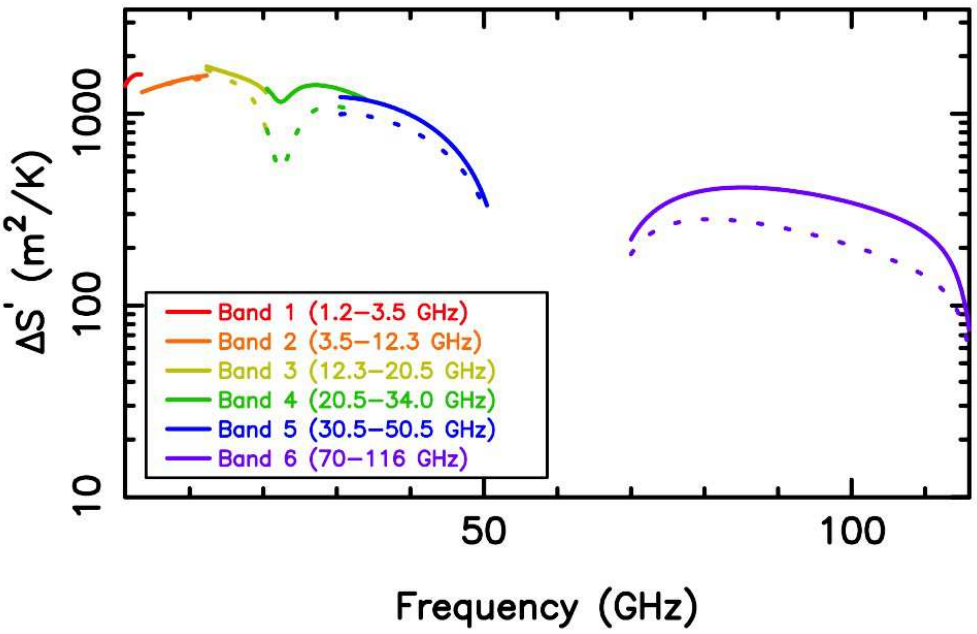

Figure 7: Spectral line sensitivity as a function of frequency for ngVLA with values for dry (solid line) and wet (dashed line) conditions for band 1 (red), band 2 (orange), band 3 (yellow), band 4 (green), band 5 (blue), and band 6 (purple).

ALMA

We use the ALMA definitions of quantities for Bands 1, 2, and 3 from Mangum et al. (2017). Specifically, we take T_{rx} = 23 K for Band 1 below 47 GHz, 32 K from 47 to 51 GHz, and T_{rx} = 37 K for Bands 2 and 3. We take T_{spill} = 13.4 K (which is appropriate for the value of η_l (0.95) and taking an ambient temperature (T_{amb}) of 269 K). We use the same atmospheric model used for the ngVLA calculation, but with a model atmosphere appropriate to the ALMA site, with 5 mm PWV ($7^{\rm th}$ octile). And we take the antenna efficiency as 0.75 across all three bands.

SKA1-mid

We define the SKA1-mid value as a sum of a contribution from the SKA1-mid (maximum of 133 dishes of 15 m diameter) and Meerkat (64 dishes of 13.5 m diameter). For both we use a model atmosphere that has 5 mm of PWV and surface temperature of 280 K for dry conditions, and 20 mm of PWV and surface temperature of 300 K for wet conditions, to determine T_{atm} and τ (at 50 degrees elevation). We use T_{bg} the same as for ngVLA. For

other values, we take the treatment given in Braun et al. (2017), described here. We use T_{spill} of 3 K for SKA1-mid and 5 K for Meerkat. We use T_{rx} values:

$T_{rx} = 7.5$ K – SKA1-mid bands 2 (0.95-1.76 GHz), 3 (1.65-3.05 GHz), and 4 (2.80-5.18 GHz)

$T_{rx} = 4.4 + 0.69\ \nu_{GHz}$ K – SKA1-mid band 5+ (4.6-50 GHz)

$T_{rx} = 6.5 + 6.8\ (|\nu_{GHz} 1.65|)^{3/2}$ K – Meerkat band L (0.9-1.67 GHz)

$T_{rx} = 9 + \nu_{GHz}$ – Meerkat band S (1.65-3.05 GHz)

And we use an antenna efficiency that is a product of three terms: η_F (feed illumination efficiency), η_D (diffraction efficiency), and η_p (phase efficiency - i.e., Ruze losses). The feed illumination efficiency is defined as $\eta_F = A_F - 0.04|\log_{10}(\nu_{GHz})|$ where $A_F = 0.92$ for SKA1-mid and 0.80 for Meerkat. The diffraction efficiency is defined as $\eta_D = 1 - 20(\lambda/D)^{3/2}$ for wavelength λ and dish diameter D. The phase efficiency is defined as in equation 3 above, with the surface error term a combination of errors in the primary (with subscript p) and secondary (with subscript s): $\sigma = \sqrt{A_p \sigma_p^2 + A_s \sigma_s^2}$, with $A_p = 0.89$, $A_s = 0.98$, $\sigma_p = 280$ μm, $\sigma_s = 154$ μm for SKA1-mid, and $A_p = 0.89$, $A_s = 0.98$, $\sigma_p = 480$ μm, $\sigma_s = 265$ μm for Meerkat. We note that the current deployment baseline of SKA1-mid has all 133 antennas outfitted only with bands 1 and 2, and 67 antennas outfitted with bands 5a and 5b (covering 4.6-15.4 GHz) see http://skatelescope.org/notes-from-the-chair/. We do not include this current deployment baseline, but rather only the baseline design that has all 133 antennas outfitted with all bands, in our analysis.

Results

Figure 8 plots $\Delta S'$ for ngVLA, VLA, ALMA, and SKA1-mid.

3.2 Frequency response considering bandwidth (continuum)

As noted, the above treatment of the frequency response is appropriate for spectral line sensitivity - where the available bandwidth is not relevant when comparing different telescopes (the assumption is that they all have sufficient frequency resolution to resolve the line and that they have enough bandwidth to encompass the entire line). However, it doesnt allow for the fact that different telescopes have different bandwidths available for continuum

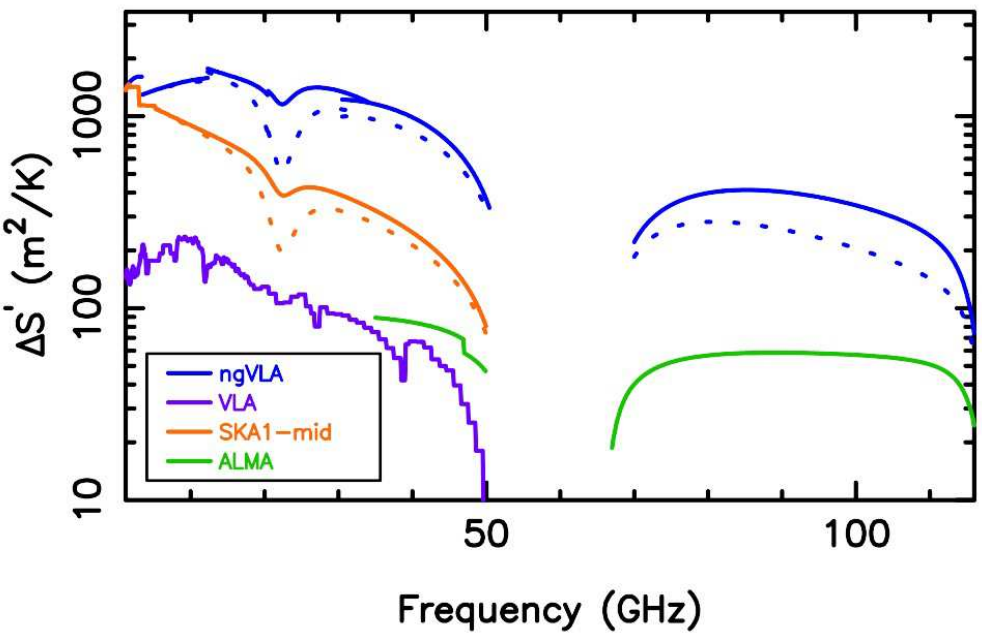

Figure 8: Spectral line sensitivity as a function of frequency for ngVLA, VLA, SKA1-mid, and ALMA. ngVLA values are plotted for dry (solid line) and wet (dashed line) conditions in blue; VLA values are plotted in purple; SKA1-mid values are plotted in orange for dry (solid line) and wet (dashed line) conditions; ALMA values are plotted in green.

observations. If we make a quantity similar to that in equation 6, but including bandwidth:

$$\Delta S''(\nu) = \frac{\sqrt{\Delta\nu} N \pi D^2 \eta_a(\nu)}{4 T_{sys}(\nu)} \qquad [\mathrm{m}^2/\sqrt{\mathrm{GHz}}/\mathrm{K}] \tag{7}$$

that will account for the available bandwidth. There are several caveats when considering such a quantity, of course, including the fact that the entire bandwidth is not available at every frequency (because of band edges and RFI). Also, for very large fractional bandwidths, the definition of sensitivity in terms of flux density (Jy) at a given frequency becomes a function of the spectral shape of the source itself. The parameter defined in equation 7 is appropriate for flat spectrum sources. Still, examination of this quantity is illuminating. For this, we assume that all four telescopes have dual polarization. For ALMA we assume $\Delta\nu$ = 8 GHz. For VLA we assume $\Delta\nu$ = 1 GHz for L-band, $\Delta\nu$ = 2 GHz for S-band, $\Delta\nu$ = 4 GHz for C- and X-bands, $\Delta\nu$ = 6 GHz for Ku-band, and $\Delta\nu$ = 8 GHz for K-, Ka-, and Q-bands. For ngVLA we assume that is the entire width of each band, except for band 6

where $\Delta\nu = 20$ GHz. For SKA1-mid, we assume that $\Delta\nu$ is 0.8 GHz for band 2, 1.0 GHz for band 3, 2.4 GHz for band 4, and 5.0 GHz for band 5+. Figure 9 plots $\Delta S''$ for ngVLA, ALMA, and SKA1-mid.

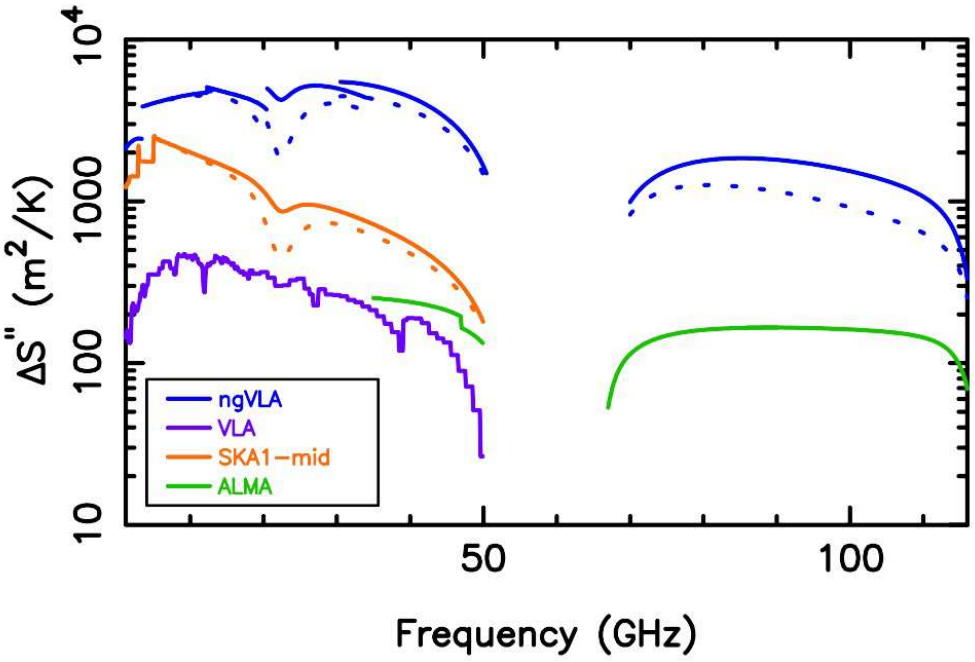

Figure 9: Continuum sensitivity as a function of frequency for ngVLA, VLA, SKA1-mid, and ALMA. ngVLA values are plotted for dry (solid line) and wet (dashed line) conditions in blue; VLA values are plotted in purple; SKA1-mid values are plotted in orange for dry (solid line) and wet (dashed line) conditions; ALMA values are plotted in green.

4 Summary

We find that the ngVLA, with its current design, is roughly a factor of 10 more sensitive than VLA and ALMA, and factor of 2-4 more sensitive than SKA1-mid (current baseline design) for spectral line observations, and a factor of 10 or more sensitive than VLA and ALMA for continuum observations, and a factor of 3-10 more sensitive than SKA1-mid for continuum observations due to increased available bandwidth. These calculations will remain under investigation as the project matures. The values presented herein represent the state of the project as it stands today, and can be used to inform studies of the scientific potential of the ngVLA.

References

Baker, L., Analysis of ngVLA Design #6 With Ideal and Actual Feed, ngVLA Document # 020.25.01.00.00-0001-REP, 2018

Baker, L., & B. Veidt, DVA-1 Performance With An Octave Horn From CST & GRASP Simulations, NRC Internal Report, 2014

Braun, R., et al., Anticipated SKA1 Science Performance, SKA Document SKA-TEL-SKO-0000818, 2017

Butler, B., Some Issues for Water Vapor Radiometry at the VLA, VLA Scientific Memo. No. 177, 1999

Butler, B., & A. Wootten, ALMA Sensitivity, Supra-THz Windows, and 20 km baselines, ALMA Memo. No. 276, 1999

Butler, B., Precipitable Water at KP 1993-1998, MMA Memo. No. 238, 1998b

Butler, B., Precipitable Water at the VLA 1990-1998, VLA Scientific Memo. No. 237, 1998a

Carilli, C., & 19 others, Science Working Groups Project Overview, ngVLA memo 5, 2015

Grammer, W., & S. Durand, Front End Reference Design Description, ngVLA Document # 020.30.03.00.00-0003-DSN, 2019

Liebe, H.J., MPM - an atmospheric millimeter-wave propagation model, International Journal of Infrared and Millimeter Waves, 10, 631650, 1989

Mangum, J., ALMA Sensitivity Metric for Science Sustainability Projects, ALMA Memo 602, 2017

Napier, P., The Primary Antenna Elements, in *Synthesis Imaging in Radio Astronomy II*, ASP press, 1998

Ruze, J., The Effect of Aperture Erros on the Antenna Radiation Pattern, Nuevo Cimento Suppl., 9, 364380, 1952

Selina, R., & E, Murphy, ngVLA Reference Design Development & Performance Estimates, ngVLA memo 17, 2017

Ulich, B.L., R.W. Haas, Absolute Calibration of Millimeter-Wavelength Spectral Lines, ApJ, 30, 247258, 1976

Weinreb, S., & H. Mani, Low Cost 1.2 to 116 GHz Receiver System - a Benchmark for ngVLA, presented at the Developing the ngVLA Science Program Workshop, 2017